Preparation and Characterization of Osmium−Stannyl Polyhydrides: d^4-d^2 Oxidative Addition of Neutral Molecules in a Late Transition Metal

Miguel A. Esteruelas,*[,‡] Agustí Lledós,*[,†] Feliu Maseras,[†] Montserrat Oliván,[‡] Enrique Oñate,[‡] María A. Tajada,[‡] and Jaume Tomàs[†]

Departamento de Química Inorgánica, Instituto de Ciencia de Materiales de Aragón, Universidad de Zaragoza-CSIC, 50009 Zaragoza, Spain, and Departament de Química, Edifici Cn, Universitat Autònoma de Barcelona, 08193 Bellaterra, Barcelona, Spain

Received December 26, 2002

Complex $OsH_2Cl_2(P^iPr_3)_2$ (**1**) reacts with 2.0 equiv of $HSnPh_3$ to give the tetrahydride-stannyl derivative $OsH_4Cl(SnPh_3)(P^iPr_3)_2$ (**2**) and $ClSnPh_3$. The structure of **2** has been determined by X-ray diffraction analysis. In the solid state and in solution at temperatures lower than 298 K, the coordination geometry around the osmium atom can be rationalized as derived from a distorted dodecahedron. In the presence of diphenylacetylene, complex **2** gives $OsH_3(SnClPh_2)\{\eta^2\text{-}CH_2{=}C(CH_3)P^iPr_2\}(P^iPr_3)$ (**3**), *cis*-stilbene, and benzene. In the solid state, the structure of **3** determined by X-ray diffraction analysis can be described as a very distorted pentagonal bipyramid, with the phosphorus atom of the triisopropylphosphine ligand and the midpoint of the olefinic bond of the isopropenyl group of the dehydrogenated phosphine occupying axial positions. In solution, at temperatures higher than 233 K, the coordinated olefin is released. Complex **3** reacts with molecular hydrogen to afford the pentahydride $OsH_5(SnClPh_2)(P^iPr_3)_2$ (**4**), as a result of the hydrogenation of the coordinated olefinic bond and the d^4-d^2 oxidative addition of hydrogen. The structure of **4** in the solid state also has been determined by X-ray diffraction. The coordination geometry around the osmium atom can be rationalized as a distorted dodecahedron. In solution, complex **4** does not have a rigid structure even at 193 K. DFT calculations in model systems of **2**, **3**, and **4**, in which the bulky ligands have been replaced by small models, followed by QM/MM optimizations with the real ligands have allowed the complete determination of the hydride positions and of the role played by steric effects in the experimental structures.

Introduction

Transition-metal hydride compounds play a central role in modern inorganic and organometallic chemistry, including chemical reactivity, instrumental investigation, theory, and applications in catalysis, biochemistry, and material science.[1]

In particular, ruthenium- and osmium-hydride complexes have proven to be useful precursors for carbon−carbon and carbon−heteroatom coupling reactions. The increase of the number of hydrogen atoms bonded to the metallic center allows the access of several organic molecules into the metal, which can be sequential and selective. In addition, a wide range of organometallic functional groups can be obtained. All this facilitates the coupling reactions and the generation of organic fragments with a rich organic chemistry, which permits the growth of the ligands.[2]

There is an emerging greater use of transition-metal tin compounds in the catalysis of organic transformations. Tin ligands have a strong labilizing effect on their trans ligands and are also quite labile themselves; thus they promote migratory insertions or provide vacant coordination sites on the transition metal by dissociation. Another reason for the use of tin compounds in catalytic cycles is the ease of oxidative addition and subsequent reductive elimination of tin(IV) compounds.[3]

We have previously shown that from the metals in the iron triad not only ruthenium but also osmium forms a variety of complexes that behave as good catalysts.[4] In an effort to join the advantages of both polyhydride and tin complexes, we are attempting to prepare novel osmium−stannyl compounds containing a high number of hydrogen atoms bonded to the metallic center.

Mononuclear stannyl complexes of osmium[5] are scarce in comparison with those of iron[6] and ruthenium.[7] With a few exceptions, such as $FeH_3(SnR_3)(PPh_2R)_3$ [6f] and $OsH_3(SnR_3)(CO)(P^iPr_3)_2$,[5b] the hydride derivatives are mono- or dihydride species. In general, they are prepared by oxidative addition of $H-SnR_3$ tin-hydrides to

‡ Universidad de Zaragoza.
† Universitat Autònoma de Barcelona.

(1) *Recent Advances in Hydride Chemistry*; Peruzzini, M., Poli, R., Eds.; Elsevier: Amsterdam, The Netherlands, 2001.
(2) Esteruelas, M. A.; López, A. M. Ruthenium- and Osmium-hydride compounds containing triisopropylphosphine as precursor for carbon−carbon and carbon−heteroatom coupling reactions. In *Recent Advances in Hydride Chemistry*; Peruzzini, M., Poli, R., Eds.; Elsevier: Amsterdam,The Netherlands, 2001; Chapter 7, pp 189−284.
(3) Holt, M. S.; Wilson, W. L.; Nelson, J. H. *Chem. Rev.* **1989**, *89*, 11.
(4) Esteruelas, M. A.; Herrero, J.; López, A. M.; Oliván, M. *Organometallics* **2001**, *20*, 3202 and references therein.

10.1021/om021038i CCC: $25.00
Publication on Web 04/05/2003

starting complexes with the metal in a low oxidation state (d^8 or d^6 ions).[3]

For the d-block elements, the group oxidation number may be achieved in elements that lie toward the left of the block but not by elements on the right. Consistent with this, the oxidative addition of neutral XY molecules to d^4 L_nM complexes of the platinum group metals to give the corresponding d^2 L_nMXY derivatives is unknown. In this context, it should be mentioned that Gusev, Berke, Caulton, and co-workers have studied the reaction of the unsaturated dihydride−dichloro−osmium(IV) complex $OsH_2Cl_2(P^iPr_3)_2$ with molecular hydrogen. Although the metal coordinates the H_2 molecule, d^2 species are not accessible.[8]

Scheme 1

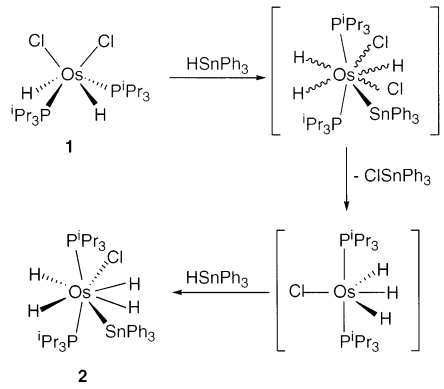

We have now observed that, in contrast to molecular hydrogen, the reaction of $OsH_2Cl_2(P^iPr_3)_2$ with H−$SnPh_3$ affords a d^2−osmium complex, which is the entry to osmium−stannyl derivatives with three, four, and even five hydrogen atoms bonded to the metal.

In this paper, we report the first oxidative additions of a neutral molecule to the d^4 platinum group metal complexes, and the synthesis and full characterization of the novel osmium−stannyl polyhydride derivatives $OsH_4Cl(SnPh_3)(P^iPr_3)_2$, $OsH_3(SnPh_2Cl)\{\eta^2\text{-}CH_2{=}C(CH_3)\text{-}P^iPr_2\}(P^iPr_3)$ and $OsH_5(SnPh_2Cl)(P^iPr_3)_2$.

Results and Discussion

1. Synthesis and Characterization of $OsH_4Cl(SnPh_3)(P^iPr_3)_2$. Treatment of toluene suspensions of $OsH_2Cl_2(P^iPr_3)_2$ (**1**) with 2.0 equiv of $HSnPh_3$ for 2 min at room temperature leads to $ClSnPh_3$ and the tetrahydride−stannyl derivative $OsH_4Cl(SnPh_3)(P^iPr_3)_2$ (**2**), which was isolated as a white solid in 52% yield.

The formation of $ClSnPh_3$, which was characterized by MS (*m*/*z* 385), suggests that **2** is the result of the elemental steps shown in Scheme 1. Initially, the oxidative addition of $HSnPh_3$ to **1** should afford the osmium(VI) intermediate $OsH_3Cl_2(SnPh_3)(P^iPr_3)_2$, which could evolve by reductive elimination of $ClSnPh_3$ into the previously reported trihydride $OsH_3Cl(P^iPr_3)_2$.[9] The oxidative addition of a second molecule of $HSnPh_3$ to this unsaturated species should give **2**.

Complex **2** was characterized by elemental analysis, IR, and ^1H, $^{31}P\{^1H\}$, $^{13}C\{^1H\}$, and $^{119}Sn\{^1H\}$ NMR spectroscopy, and by an X-ray crystallographic study. At 173 K, the hydrogen atoms H(01), H(02), H(03), and H(04) were located in the difference Fourier maps and refined as isotropic atoms together with the remaining non-hydrogen atoms of the structure. A view of the molecular geometry of **2** is shown in Figure 1. Selected bond distances and angles are listed in Table 1.

(5) For osmium complexes reported before 1989 see ref 3, while for osmium complexes reported since 1989 see: (a) Clark, G. R.; Flower, K. R.; Rickard, C. E. F.; Roper, W. R.; Salter, D. M.; Wright, L. J. *J. Organomet. Chem.* **1993**, *462*, 331. (b) Buil, M. L.; Espinet, P.; Esteruelas, M. A.; Lahoz, F. J.; Lledós, A.; Martínez-Ilarduya, J. M.; Maseras, F.; Modrego, J.; Oñate, E.; Oro, L. A.; Sola, E.; Valero, C. *Inorg. Chem.* **1996**, *35*, 1250. (c) Clark, A. M.; Rickard, C. E. F.; Roper, W. R.; Wright, L. J. *J. Organomet. Chem.* **1997**, *543*, 111. (d) Rickard, C. E. F.; Roper, W. R.; Woodman, T. J.; Wright, L. J. *Chem. Commun.* **1999**, 1101. (e) Rickard, C. E. F.; Roper, W. R.; Woodman, T. J.; Wright, L. J. *Chem. Commun.* **1999**, 837. (f) Baya, M.; Crochet, P.; Esteruelas, M. A.; Gutiérrez-Puebla, E.; Ruiz, N. *Organometallics* **1999**, *18*, 5034. (g) Möhlen, M.; Rickard, C. E. F.; Roper, W. R.; Salter, D. M.; Wright, L. J. *J. Organomet. Chem.* **2000**, *593*−*594*, 458. (h) Clark, A. M.; Rickard, C. E. F.; Roper, W. R.; Woodman, T. J.; Wright, L. J. *Organometallics* **2000**, *19*, 1766.

(6) For iron complexes reported before 1989 see ref 3, while for iron complexes reported since 1989 see: (a) Knorr, M.; Piana, H.; Gilbert, S.; Schubert, U. *J. Organomet. Chem.* **1990**, *388*, 327. (b) Lee, S. S.; Knobler, C. B.; Hawthorne, M. F. *Organometallics* **1991**, *10*, 1054. (c) Akita, M.; Oku, T.; Tanaka, M.; Moro-oka, Y. *Organometallics* **1991**, *10*, 3080 (d) Pannell, K.; Castillo-Ramirez, J.; Cervantes-Lee, F. *Organometallics* **1992**, *11*, 3139. (e) Schubert, U.; Grubert, S.; Schulz, U.; Mock, S. *Organometallics* **1992**, *11*, 3163 (f) Schubert, U.; Gilbert, S.; Mock, S. *Chem. Ber.* **1992**, *125*, 835. (g) Schubert, U.; Gilbert, S.; Knorr, M. *J. Organomet. Chem.* **1993**, *454*, 79. (h) Veith, M.; Stahl, L.; Huch, V. *Organometallics* **1993**, *12*, 1914. (i) Chang, S.; White, P. S.; Brookhart, M. *Organometallics* **1993**, *12*, 3636. (j) Gordon, C.; Schubert, U. *Inorg. Chim. Acta* **1994**, *224*, 177. (k) Braunstein, P.; Knorr, M.; Strampfer, M.; DeCian, A.; Fischer, J. *J. Chem. Soc., Dalton Trans.* **1994**, 117. (l) Gilbert, S.; Knorr, M.; Mock, S.; Schubert, U. *J. Organomet. Chem.* **1994**, *480*, 241. (m) Hellmann, K. W.; Friedrich, S.; Gade, L. H.; Li, W.-S.; McPartlin, M. *Chem. Ber.* **1995**, *128*, 29. (n) Adams, H.; Maloney, C. A.; Muir, J. E.; Walters, S. J.; Winter, M. J. *J. Chem. Soc., Chem. Commun.* **1995**, 1511. (o) Kay, M.; Mackay, K. M.; Nicholson, B. K. *J. Organomet. Chem.* **1995**, *491*, 247. (p) Braunstein, P.; Charles, C.; Tiripicchio, A.; Ugozzoli, F. *J. Chem. Soc., Dalton Trans.* **1996**, 4365. (q) He, X.; Hartwig, J. F. *Organometallics* **1996**, *15*, 400. (r) Nakazawa, H.; Yamaguchi, Y.; Miyoshi, K. *Organometallics* **1996**, *15*, 1337. (s) Schubert, U.; Grubert, S. *Organometallics* **1996**, *15*, 4707. (t) Braunstein, P.; Charles, C.; Kickelbick, G.; Schubert, U. *Chem. Commun.* **1997**, 1911. (u) McArdle, P.; Ryder, A. G.; Cunningham D. *Organometallics* **1997**, *16*, 2638. (v) Nakazawa, H.; Yamaguchi, Y.; Kawamura, K.; Miyoshi, K. *Organometallics* **1997**, *16*, 4626. (w) Adams, H.; Broughton, S. G.; Walters, S. J.; Winter, M. J. *Chem. Commun.* **1999**, 1231.

(7) For some representative examples of Ru−stannyl complexes see: (a) Cabeza, J. A.; Llamazares, A.; Riera, V.; Triki, S.; Ouahab, L. *Organometallics* **1992**, *11*, 3334. (b) Clark, G. R.; Flower, K. R.; Roper, W. R.; Wright, L. J. *Organometallics* **1993**, *12*, 259. (c) Clark, G. R.; Flower, K. R.; Roper, W. R.; Wright, L. J. *Organometallics* **1993**, *12*, 3810. (d) Cabeza, J. A.; García-Granda, S.; Llamazares, A.; Riera, V.; Van der Maelen, J. F. *Organometallics* **1993**, *12*, 157. (e) Buil, M. L.; Esteruelas, M. A.; Lahoz, F. J.; Oñate, E.; Oro, L. A. *J. Am. Chem. Soc.* **1995**, *117*, 3619. (f) Rudd, J. A., II; Angelici, R. J. *Inorg. Chim. Acta* **1995**, *240*, 393. (g) Moreno, B.; Sabo-Etienne, S.; Dahan, F.; Chaudret, B. *J. Organomet. Chem.* **1995**, *498*, 139. (h) Cardin, C. J.; Cardin D. J.; Convery, M. A.; Dauter, Z.; Fenske, D.; Devereux, M. M.; Power, M. B. *J. Chem. Soc., Dalton Trans.* **1996**, *1133*. (i) Akita, M.; Hua, R.; Oku, T.; Tanaka, M.; Moro-oka, Y. *Organometallics* **1996**, *15*, 4162. (j) Aarnts, M. P.; Wilms, M. P.; Peelen, K.; Fraanje, J.; Goubitz, K.; Hartl, F.; Stufkens, D. J.; Baerends, E. J.; Vlĉek, A., Jr. *Inorg. Chem.* **1996**, *35*, 5468. (k) Aarnts, M. P.; Stufkens, D. J.; Oskam, A.; Fraanje, J.; Goubitz, K. *Inorg. Chim. Acta* **1997**, *256*, 93. (l) Akita, M.; Hua, R.; Nakaniski, S.; Tanaka, M.; Moro-oka, Y. *Organometallics* **1997**, *16*, 5572. (m) Aarnts, M. P.; Oskam, A.; Stufkens, D. J.; Fraanje, J.; Goubitz, K.; Veldman, N.; Spek, A. L. *J. Organomet. Chem.* **1997**, *531*, 191. (n) Bois, C.; Cabeza, J. A.; Franco, R. J.; Riera, V.; Soborit, E. *J. Organomet. Chem.* **1998**, *564*, 201. (o) Kawamura, K.; Nakazawa, H.; Miyoshi, K. *Organometallics* **1999**, *18*, 4785. (p) Hermans, S.; Johnson, B. F. G. *Chem. Commun.* **2000**, 1955. (q) Rosa, P.; Mézailles, N.; Ricard, L.; Mathey, F.; Le Floch, P.; Jean, Y. *Angew. Chem., Int. Ed.* **2001**, *40*, 1251.

(8) (a) Gusev, D. G.; Kuznetsov, V. F.; Eremenko, I. L.; Berke, H. *J. Am. Chem. Soc.* **1993**, *115*, 5831. (b) Kuhlman, R.; Gusev, D. G.; Eremenko, I. L.; Berke, H.; Huffman, J. C.; Caulton, K. G. *J. Organomet. Chem.* **1997**, *536*−*537*, 139.

(9) (a) Gusev, D. G.; Kuhlman, R.; Sini, G.; Eisenstein, O.; Caulton, K. G. *J. Am. Chem. Soc.* **1994**, *116*, 2685. (b) Kuhlman, R.; Clot, E.; Leforestier, C.; Streib, W. E.; Eisenstein, O.; Caulton, K. G. *J. Am. Chem. Soc.* **1997**, *119*, 10153.

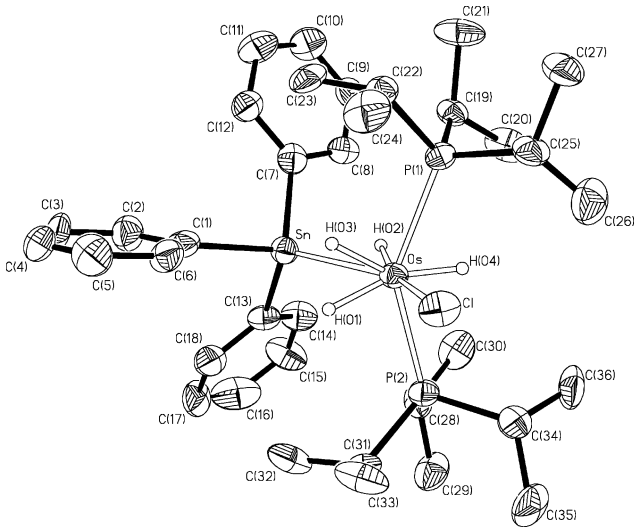

Figure 1. Molecular diagram of complex $OsH_4Cl(SnPh_3)(P^iPr_3)_2$ (**2**).

Table 1. Selected Bond Distances and Angles for the Complex $OsH_4Cl(SnPh_3)(P^iPr_3)_2$ (2) and Optimized Distances and Angles of $OsH_4Cl(SnH_3)(PH_3)_2$ (2a, B3LYP) and $OsH_4Cl(SnPh_3)(P^iPr_3)_2$ (2b, IMOMM (B3LYP:MM3)) (distances in Å, Angles in deg)

	2	2a	2b
Os−Sn	2.6691(7)	2.713	2.742
Os−P(1)	2.394(2)	2.361	2.451
Os−P(2)	2.406(2)	2.365	2.460
Os−Cl	2.4710(19)	2.518	2.536
Os−H(01)	1.42(6)	1.646	1.630
Os−H(02)	1.55(6)	1.633	1.629
Os−H(03)	1.47(6)	1.639	1.624
Os−H(04)	1.34(6)	1.665	1.657
Sn···H(01)		2.667	2.609
Sn···H(02)		2.298	2.277
Sn···H(03)		2.684	2.635
H(01)···H(03)		1.671	1.766
Sn−Os−P(1)	102.89(5)	99.853	104.637
Sn−Os−P(2)	101.14(6)	98.914	102.630
Sn−Os−Cl	145.43(5)	148.294	142.335
Sn−Os−H(01)	65(2)	70.651	67.852
Sn−Os−H(02)	44(2)	57.609	56.070
Sn−Os−H(03)	66(2)	71.357	68.836
Sn−Os−H(04)	126(2)	129.940	130.657
P(1)−Os−P(2)	145.05(7)	151.176	142.377
P(1)−Os−Cl	85.90(7)	87.989	85.659
P(2)−Os−Cl	88.52(7)	87.437	88.369
P(1)−Os−H(01)	130(3)	135.142	139.573
P(1)−Os−H(02)	83(2)	86.000	85.849
P(1)−Os−H(03)	80(2)	74.145	74.486
P(1)−Os−H(04)	68(2)	73.847	71.165
P(2)−Os−H(01)	83(2)	72.155	75.313
P(2)−Os−H(02)	97(2)	85.802	88.332
P(2)−Os−H(03)	134(2)	133.035	140.529
P(2)−Os−H(04)	78(2)	77.332	71.448
Cl−Os−H(01)	83(2)	82.092	80.780
Cl−Os−H(02)	168(2)	154.084	161.447
Cl−Os−H(03)	83(2)	81.592	79.763
Cl−Os−H(04)	88(2)	81.765	87.009
H(01)−Os−H(02)	108(3)	119.206	115.917
H(01)−Os−H(03)	51(3)	61.174	65.717
H(01)−Os−H(04)	159(3)	145.932	144.815
H(02)−Os−H(03)	101(3)	120.606	113.647
H(02)−Os−H(04)	82(3)	72.347	74.639
H(03)−Os−H(04)	147(3)	144.238	143.949

The coordination geometry around the osmium atom can be rationalized as derived from a distorted dodecahedron. This dodecahedral structure is defined by two intersecting orthogonal (88(2)°) trapezoidal planes. One plane contains the atoms P(1), H(03), H(01), and P(2) with a P(1)−Os−P(2) angle of 145.05(7)°. The second trapezoidal plane contains the atoms Sn, H(02), H(04), and Cl with a Cl−Os−Sn angle of 145.43(5)°. Similar structures have been found for the hexahydride $OsH_6(P^iPr_2Ph)_2$[10] and the pentahydrides $[OsH_5(PHPh_2)(P^iPr_3)_2]^+$[11] and $[OsH_5(PMe_2Ph)_3]^+$.[12] In addition, the Y-shape of the OsP_2Sn skeleton should be noted, where the P(1)−Os−Sn and P(2)−Os−Sn angles are 102.89(5)° and 101.14(6)°.

In general, the hydride positions obtained from X-ray diffraction data are imprecise.[13] However, DFT calculations have been shown to provide useful accurate data for the hydrogen position in both classical polyhydride[14] and dihydrogen complexes.[15] So, to corroborate the structure of **2**, a DFT study of the model complex $OsH_4Cl(SnH_3)(PH_3)_2$ (**2a**), supplemented by QM/MM IMOMM calculations on the real complex, has been carried out.

Figure 2a shows the B3LYP optimized structure of $OsH_4Cl(SnH_3)(PH_3)_2$ (**2a**), while Figure 2b shows the IMOMM (B3LYP:MM3) optimized structure of **2** (**2b**). Their main geometrical parameters are listed in Table 1. Both theoretical results agree well with the dodecahedral structure obtained from the X-ray diffraction experiment, and two almost perpendicular trapezoidal planes are found. Overall, the geometrical parameters of **2a** and **2b** are similar, indicating that the steric hindrance of the bulky ligands does not produce any severe distortion in the coordination polyhedron. However, some subtle differences are found. As expected, a better agreement with the X-ray diffraction data is obtained in the QM/MM calculations, specially in the bond angles. For instance, the angle P−Os−P is 151.2° in **2a** and 142.3 in **2b**, whereas the experimental value is 145.05(7)°. It could seem a bit surprising that a larger P−Os−P bond angle is found for PH_3 than for the bulkier P^iPr_3. The same happens with the Sn−Os−Cl angle (148.3° in **2a** and 142.3 in **2b**). The answer for

(10) Howard, J. A. K.; Johnson, O.; Koetzle, T. F.; Spencer, J. L. *Inorg. Chem.* **1987**, *26*, 2930.
(11) Esteruelas, M. A.; Lledós, A.; Martin, M.; Maseras, F.; Osés, R.; Ruiz, N.; Tomás, J. *Organometallics* **2001**, *20*, 5297.
(12) (a) Johnson, T. S.; Huffman, J. C.; Caulton, K. G.; Jackson, S. A.; Eisenstein, O. *Organometallics* **1989**, *8*, 2073. (b) Johnson, T. J.; Albinati, A.; Koetzle, T. F.; Ricci, J. Eisenstein, O.; Huffman, J. C.; Caulton, K. G. *Inorg. Chem.* **1994**, *33*, 4966.
(13) Zhao, D.; Bau, R. *Inorg. Chim. Acta* **1998**, *269*, 162.
(14) See for example: (a) Lin, Z.; Hall, M. B. *Inorg. Chem.* **1991**, *30*, 2569. (b) Lin, Z.; Hall, M. B. *Coord. Chem. Rev.* **1994**, *135*, 845. (c) Esteruelas, M. A.; Jean, Y.; Lledós, A.; Oro, L. A.; Ruiz, N.; Volatron, F. *Inorg. Chem.* **1994**, *33*, 3609. (d) Camanyes, S.; Maseras, F.; Moreno, M.; Lledós, A.; Lluch, J. M.; Bertrán, J. *J. Am. Chem. Soc.* **1996**, *118*, 4617. (e) Demachy, I.; Esteruelas, M. A.; Jean, Y.; Lledós, A.; Maseras, F.; Oro, L. A.; Valero, C.; Volatron, F. *J. Am. Chem. Soc.* **1996**, *118*, 8388. (f) Castillo, A.; Barea, G.; Esteruelas, M. A.; Lahoz, F. J.; Lledós, A.; Maseras, F.; Modrego, J.; Oñate, E.; Oro, L. A.; Ruiz, N.; Sola, E. *Inorg. Chem.* **1999**, *38*, 1814. (g) Buil, M. L.; Esteruelas, M. A.; Modrego, J.; Oñate, E. *New J. Chem.* **1999**, *23*, 403. (h) Castarlenas, R.; Esteruelas, M. A.; Gutiérrez-Puebla, E.; Jean, Y.; Lledós, A.; Martín, M.; Tomás, J. *Organometallics* **1999**, *18*, 4296. (i) Maseras, F.; Lledós, A.; Clot, E.; Eisenstein, O. *Chem. Rev.* **2000**, *100*, 601.
(15) See for example: (a) Dapprich, S.; Frenking, G. *Angew. Chem., Int. Ed. Engl.* **1995**, *24*, 354. (b) Bakhmutov, V. I.; Bertrán, J.; Esteruelas, M. A.; Lledós, A.; Maseras, F.; Modrego, J.; Oro, L. A.; Sola, E. *Chem. Eur. J.* **1996**, *2*, 815. (c) Maseras, F.; Lledós, A.; Costas, M.; Poblet, J. M. *Organometallics* **1996**, *15*, 2947. (d) Gelabert, R.; Moreno, M.; Lluch, J. M.; Lledós, A. *Organometallics* **1997**, *16*, 3805. (e) Albéniz, M. J.; Esteruelas, M. A.; Lledós, A.; Maseras, F.; Oñate, E.; Oro, L. A.; Sola, E.; Zeier, B. *J. Chem. Soc., Dalton Trans.* **1997**, *181*. (f) Barea, G.; Esteruelas, M. A.; Lledós, A.; López, A. M.; Oñate, E.; Tolosa, J. I. *Organometallics* **1998**, *17*, 4065. (g) Barea, G.; Esteruelas, M. A.; Lledós, A.; López, A. M.; Tolosa, J. I. *Inorg. Chem.* **1998**, *37*, 5033.

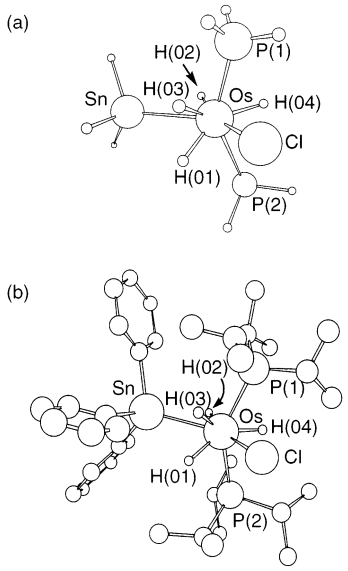

Figure 2. (a) B3LYP optimized structure of $OsH_4Cl(SnH_3)(PH_3)_2$ (**2a**) and (b) IMOMM (B3LYP:MM3) optimized structure of $OsH_4Cl(SnPh_3)(P^iPr_3)_2$ (**2b**).

this behavior is found in the Sn−Os−P angles, which become larger in **2b**, thus minimizing the repulsions between the phosphine and stannyl substituents.

As expected the Os−H distances are between 1.62 and 1.66 Å, while the separation between the hydride ligands is in all cases longer than 1.7 Å. This clearly supports the tetrahydride character of **2**. Neither is there any interaction between the tin atom and the hydride ligands. Although the separation Sn−H(2) (2.298 and 2.277 Å for **2a** and **2b**, respectively) is about 0.3 Å shorter than the separations in Sn−H(1) (2.667 Å in **2a** and 2.609 Å in **2b**) and Sn−H(3) (2.684 and 2.635 Å for **2a** and **2b**), it is between 0.6 and 0.4 Å longer than the bond length in tin−hydride compounds of the type $H-SnR_3$.[16] In agreement with the complete addition of the H−Sn bond of $H-SnPh_3$ to the osmium atom, the Os−Sn distances (2.6691(7) Å (**2**), 2.742 (**2b**)) agree well with those reported for other mononuclear osmium−stannyl derivatives (2.6−2.7 Å),[5c,h] while they are about 0.1 Å shorter than the Os(*μ*-H)Sn osmium−tin bond length in the cluster $[Os_3SnH_2(CO)_{10}\{CH(SiMe_3)_2\}_2]$ (2.855(3) Å).[17]

The IR and the $^{31}P\{^1H\}$ NMR spectrum of **2** are consistent with the structure shown in Figures 1 and 2. The IR spectrum in Nujol contains two strong ν(Os−H) vibrations at 2083 and 1980 cm^{-1}, whereas the $^{31}P\{^1H\}$ NMR spectrum in toluene-d_8 shows a singlet at 32.5 ppm, along with the tin satellites ($J_{P-^{119}Sn} = J_{P-^{117}Sn}$ = 20 Hz). This spectrum is temperature invariant between 298 and 193 K.

In contrast with the $^{31}P\{^1H\}$ NMR spectrum, the ^1H NMR spectrum in toluene-d_8 is temperature dependent. At 298 K, the spectrum shows in the hydride region a single broad resonance at −7.71 ppm. This observation is consistent with the operation of thermally activated exchange processes for the hydride ligands, which proceed at rates sufficient to lead to the single hydride resonance. Consistent with this, lowering the sample temperature leads to broadening of the resonance. At 253 K, decoalescence occurs, and at 213 K the expected ABCC′XX′ spin system is observed (δ −2.92 part A; δ −5.92 part CC′; δ −16.01 part B). Tin satellites are not observed.

The T_1 values of the hydrogen nuclei of the OsH_4 unit of **2** were also determined over the temperature range 273−213 K. In agreement with the tetrahydride character of **2**, at 300 MHz, $T_{1(min)}$ values of 175 ± 18 (H_A), 169 ± 1 (H_C and $H_{C'}$), and 171 ± 17 ms (H_B) were obtained at 233 K. At 293 K, the $^{119}Sn\{^1H\}$ NMR spectrum shows a broad resonance centered at −88.9 ppm.

2. Synthesis and Characterization of $OsH_3(SnPh_2Cl)\{\eta^2\text{-}CH_2{=}C(CH_3)P^iPr_2\}(P^iPr_3)$. Complex **2** reacts with diphenylacetylene in toluene at room temperature to give, after 4 h, benzene, *cis*-stilbene, and the trihydride derivative $OsH_3(SnPh_2Cl)\{\eta^2\text{-}CH_2{=}C(CH_3)P^iPr_2\}(P^iPr_3)$ (**3**), which was isolated as a yellow solid in 49% yield, according to eq 1.

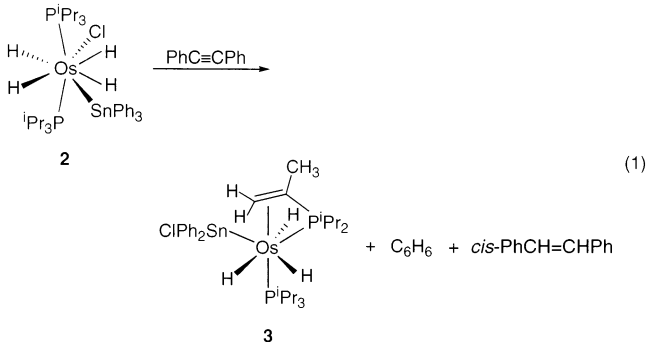

(1)

The formation of **3** is a one-pot synthesis of multiple complex reactions, which has no precedent in organometallic chemistry. Four different processes are assembled to give rise to **3**: (i) dehydrogenation of one isopropyl group of one phosphine, (ii) reduction of diphenylacetylene to give *cis*-stilbene, (iii) hydrogenolysis of a phenyl group of the triphenylstannyl ligand, and (iv) migration of the chlorine ligand from the osmium atom to the tin atom. The elemental steps of this synthesis appear to occur with the participation of radical-like species as intermediates. Thus, it should be mentioned that in the presence of hydroquinone, the formation of **3** is inhibited, and complex **2** decomposes to an ill-defined black solid.

The dehydrogenation of triisopropylphosphine together with the reduction of diphenylacetylene can be formally described as a hydrogen transfer reaction from an alkane to an unsaturated organic substrate.[18] In this context, it should be noted that the dehydrogenation of coordinated cycloalkylphosphines is a well-known process.[19] However, the dehydrogenation of acyclic alkylphosphines to give α-vinylphosphines is rare. We have previously observed that complex **1** reacts with 2.0 equiv of 1,5-cyclooctadiene and 2,5-norbornadiene to give 1.0 equiv of the corresponding monoolefin and the isopropenylphosphine derivatives $OsCl_2(diolefin)\{\eta^2\text{-}CH_2{=}C-$

(16) (a) Schager, F.; Goddard, R.; Seevogel, K.; Pörschke, K.-R. *Organometallics* **1998**, *17*, 1546. (b) Schumann, H.; Wassermann, B. C.; Frackowiak, M.; Omotowa, B.; Schutte, S.; Velder, J.; Mühle, S. H.; Krause, W. *J. Organomet. Chem.* **2000**, *609*, 189. (c) Sasaki, K.; Kondo, Y.; Maruoka, K. *Angew. Chem., Int. Ed.* **2001**, *40*, 411.

(17) Cardin, C. J.; Cardin, D. J.; Parge, H. E.; Power, J. M. *J. Chem. Soc., Chem. Commun.* **1984**, *609*.

$(CH_3)P^iPr_2\}$ (diolefin = COD, NBD).[20] Transition metal complexes containing $R_2PC(R')=CH_2$ ligands are relatively scarce. These groups act as a monodentate ligand,[21] a bridge to two metal centers,[22] and a chelating ligand.[23] Complex **3** is a rare example of the latter type of compounds, in osmium chemistry.

With regard to the hydrogenolysis of the phenyl group of the stannyl ligand and to the migration of the chlorine, we note that Roper and co-workers have previously observed a chlorine−methyl exchange in the complex $OsCl(SnMe_3)(CO)(PPh_3)_2$, promoted by pyridine.[5d]

Complex **3** was characterized by elemental analysis, IR, and ^1H, $^{31}P\{^1H\}$, $^{13}C\{^1H\}$, and $^{119}Sn\{^1H\}$ NMR spectroscopy, and by an X-ray crystallographic study, as **2**. At 173 K, the hydrogen atoms H(01), H(02), and H(03) were also located in the difference Fourier maps and refined as isotropic atoms together with the remaining non-hydrogen atoms of the structure. Figure 3 shows a view of the structure of this compound. Selected bond distances and angles are collected in Table 2.

The coordination geometry around the osmium atom can be rationalized as a very distorted pentagonal bipyramid with the phosphorus atom P(2) and the midpoint of the olefinic C(1)−C(2) bond (M) occupying axial positions (P(2)−Os−M = 165.2°). The osmium sphere is completed by the hydride ligands and the atoms Sn and P(1), which lie in the equatorial plane. The Sn atom is disposed between the hydride ligands H(03) and H(01), whereas the P(1) atom is disposed between the hydride ligands H(01) and H(02). The distortion is mainly due to the ring constraint imposed by the bidentate isopropenylphosphine ligand, which acts with a bite angle of 57.4° (P(1)−Os−M), inducing the displacement out of the equatorial plane of the P(1) atom.

The olefinic bond of the isopropenylphosphine ligand coordinates to the osmium atom in an asymmetrical

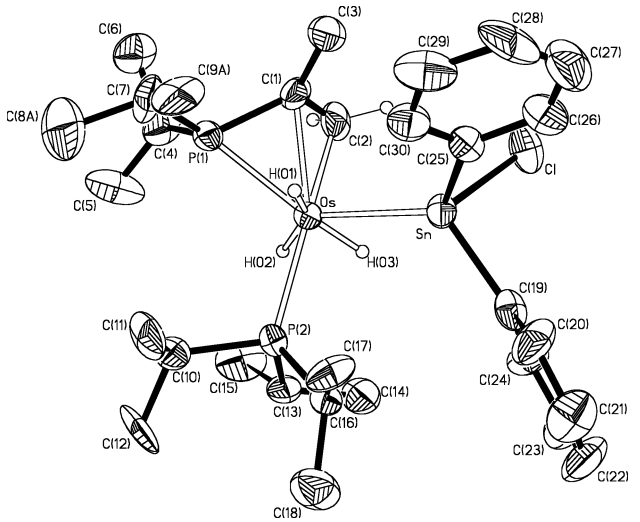

Figure 3. Molecular diagram of complex $OsH_3(SnPh_2Cl)\{\eta^2\text{-}CH_2=C(CH_3)P^iPr_2\}(P^iPr_3)$ (**3**).

fashion, with Os−C distances of 2.183(9) Å (Os−C(2)) and 2.231(10) Å (Os−C(1)). These bond lengths agree well with those found in other osmium−olefin complexes (between 2.13 and 2.28 Å).[12b,20,24] Similarly, the olefinic bond distance C(1)−C(2) (1.378(14) Å) is within the range reported for transition metal olefin complexes (between 1.340 and 1.445 Å).[25] The P(1)−C(1) distance (1.768(11) Å) is between 0.03 and 0.06 Å shorter than the P(1)−C(4) (1.836(10) Å) and P(1)−C(7) (1.800(10) Å) bond lengths. In accordance with the sp^2 hybridization for C(1), the angles P(1)−C(1)−C(3) and C(2)−C(1)−C(3) are 124.5(9)° and 122.3(10)°, respectively.

The OsP_2Sn skeleton has a Y-shape, with the osmium atom situated in the common vertex, as in **2**. However, in this case, the three angles are different: 133.08(7)° (Sn−Os−P(1)), 112.74(10)° (P(1)−Os−P(2)), and 101.99(7)° (Sn−Os−P(2)). The Os−P(1), Os−P(2), and Os−Sn distances are 2.324(3), 2.349(3), and 2.6113(8) Å, respectively.

To corroborate the structure of **3**, a DFT study of the $OsH_3(SnH_2Cl)\{\eta^2\text{-}CH_2=C(CH_3)PH_2\}(PH_3)$ (**3a**) model complex, supplemented by QM/MM IMOMM calculations on the real system, was also carried out. Figure 4a shows the B3LYP optimized structure of $OsH_3(SnH_2Cl)\{\eta^2\text{-}CH_2=C(CH_3)PH_2\}(PH_3)$ (**3a**), while Figure 4b shows the IMOMM (B3LYP/MM3) optimized structure of **3** (**3b**). Their main geometrical parameters are collected in Table 2. Both theoretical results agree well with those obtained from the X-ray diffraction experiment. Furthermore, the comparison between the structural parameters of **3a** and **3b** indicates that the steric hindrance of the bulky ligands is not responsible for the distortion in the coordination polyhedron.

The separation between the hydride ligands H(02) and H(03) is 1.951 Å for **3a** and 2.018 Å for **3b**. These

(18) (a) Crabtree, R. H. *Chem. Rev.* **1985**, *85*, 245. (b) Burk, M. J.; Crabtree, R. H. *J. Am. Chem. Soc.* **1987**, *109*, 8025. (c) Aoki, T.; Crabtree, R. H. *Organometallics* **1993**, *12*, 294. (d) Chaloner, P. A.; Esteruelas, M. A.; Joó, F.; Oro, L. A. *Homogeneous Hydrogenation*; Kluwer Academic Publisher: Dordrecht, The Netherlands, 1994; Chapter 2. (e) Jensen, C. M. *Chem. Commun.* **1999**, 2443. (f) Morales-Morales, D.; Lee, D. W.; Wang, Z.; Jensen, C. M. *Organometallics* **2001**, *20*, 1144.

(19) See for example: (a) Hietkamp, S.; Stufkens, D. J.; Vrieze, K. *J. Organomet. Chem.* **1978**, *152*, 347. (b) Arliguie, T.; Chaudret, B.; Jalon, F.; Lahoz, F. J. *J. Chem. Soc., Chem. Commun.* **1988**, *998*. (c) Campion, B. K.; Heyn, R. H.; Tilley, T. D.; Rheingold, A. L. *J. Am. Chem. Soc.* **1993**, *115*, 5527. (d) Christ, M. L.; Sabo-Etienne, S.; Chaudret, B. *Organometallics* **1995**, *14*, 1082.

(20) Edwards, A. J.; Esteruelas, M. A.; Lahoz, F. J.; López, A. M.; Oñate, E.; Oro, L. A.; Tolosa, J. I. *Organometallics* **1997**, *16*, 1316.

(21) See for example: (a) Holt, M. S.; Nelson, J. H.; Alcock, N. W. *Inorg. Chem.* **1986**, *25*, 2288. (b) Rahn, J. A.; Holt, M. S.; O'Neil-Johnson, M.; Nelson, J. H. *Inorg. Chem.* **1988**, *27*, 1316. (c) Rahn, J. A.; Delian, A.; Nelson, J. H. *Inorg. Chem.* **1989**, *28*, 215. (d) Rahn, J. A.; Holt, M. S.; Gray, G. A.; Alcock, N. W.; Nelson, J. H. *Inorg. Chem.* **1989**, *28*, 217. (e) Bhaduri, D.; Nelson, J. H.; Day, C. L.; Jacobson, R. A.; Solujić, L.; Milosavljević, E. B. *Organometallics* **1992**, *11*, 4069. (f) Adams, H.; Bailey, N. A.; Blenkiron, P.; Morris, M. J. *J. Organomet. Chem.* **1993**, *460*, 73. (g) Knox, S. A. R.; Morton, D. A. V.; Orpen, A. G.; Turner, M. L. *Inorg. Chim. Acta* **1994**, *220*, 201.

(22) See for example: (a) Wilson, W. L.; Nelson, J. H.; Alcock, N. W. *Organometallics* **1990**, *9*, 1699. (b) Hogarth, G. *J. Organomet. Chem.* **1991**, *407*, 91. (c) Doyle, M. J.; Duckworth, T. J.; Manojlović-Muir, L.; Mays, M. J.; Raithby, P. R.; Robertson, F. J. *J. Chem. Soc., Dalton Trans.* **1992**, *2703*. (d) Acum, G. A.; Mays, M. J.; Raithby, P. R.; Solan, G. A. *J. Organomet. Chem.* **1996**, *508*, 137.

(23) (a) Mercier, F.; Hugel-Le Goff, C.; Ricard, L.; Mathey, F. *J. Organomet. Chem.* **1990**, *389*, 389. (b) Mathey, F. *J. Organomet. Chem.* **1990**, *400*, 149. (c) Ji, H.; Nelson, J. H.; DeCian, A.; Fischer, J.; Solujić, L.; Milosavljević, E. B. *Organometallics* **1992**, *11*, 401.

(24) (a) Edwards, A. J.; Elipe, S.; Esteruelas, M. A.; Lahoz, F. J.; Oro, L. A.; Valero, C. *Organometallics* **1997**, *16*, 3828. (b) Esteruelas, M. A.; García-Yebra, C.; Oliván, M.; Oñate, E. *Organometallics* **2000**, *19*, 3260. (c) Baya, M.; Esteruelas, M. A.; Oñate, E. *Organometallics* **2002**, *21*, 5681.

(25) Allen, F. H.; Daris, J. E.; Galloy, J. J.; Johnson, O.; Kennard, O.; Macrae, C. F.; Mitchell, E. M.; Mitchell, G. F.; Smith, J. M.; Watson, D. G. *J. Chem. Inf. Comput. Sci.* **1991**, *31*, 187.

Table 2. Selected Bond Distances and Angles for the Complex $OsH_3(SnPh_2Cl)\{\eta^2\text{-}CH_2{=}C(CH_3)P^iPr_2\}(P^iPr_3)$ (3) and Optimized Distances and Angles of $OsH_3(SnH_2Cl)\{\eta^2\text{-}CH_2{=}C(CH_3)PH_2\}(PH_3)$ (3a, B3LYP) and $OsH_3(SnPh_2Cl)\{\eta^2\text{-}CH_2{=}C(CH_3)P^iPr_2\}(P^iPr_3)$ (3b, IMOMM (B3LYP:MM3)) (distances in Å, Angles in deg)

	3	3a	3b
Os−Sn	2.6113(8)	2.657	2.673
Os−P(1)	2.324(3)	2.397	2.441
Os−P(2)	2.349(3)	2.334	2.397
Os−C(1)	2.231(10)	2.262	2.246
Os−C(2)	2.183(9)	2.269	2.234
Os−H(01)	1.28(7)	1.683	1.672
Os−H(02)	1.55(7)	1.664	1.657
Os−H(03)	1.29(8)	1.631	1.625
Sn−Cl	2.432(3)	2.407	2.421
Sn···H(01)		2.424	2.395
Sn···H(03)		2.500	2.528
C(1)−C(2)	1.378(14)	1.417	1.425
H(02)···H(03)		1.951	2.018
Sn−Os−P(1)	133.08(7)	129.403	126.929
Sn−Os−P(2)	101.99(7)	98.234	103.628
Sn−Os−H(01)	75(3)	63.305	61.952
Sn−Os−H(02)	132(3)	138.978	142.486
Sn−Os−H(03)	59(3)	66.390	66.979
P(1)−Os−P(2)	112.74(10)	114.086	114.560
P(1)−Os−H(01)	69(3)	82.422	84.393
P(1)−Os−H(02)	92(3)	86.779	83.875
P(1)−Os−H(03)	158(4)	148.922	148.913
P(2)−Os−H(01)	98(4)	83.039	86.500
P(2)−Os−H(02)	68(3)	79.084	76.031
P(2)−Os−H(03)	77(4)	85.150	83.333
H(01)−Os−H(02)	151(4)	153.168	152.543
H(01)−Os−H(03)	131(5)	125.714	123.514
H(02)−Os−H(03)	73(4)	72.609	75.844
P(1)−C(1)−C(2)	113.0(8)	112.193	111.084
P(1)−C(1)−C(3)	124.5(9)	123.532	128.076
C(2)−C(1)−C(3)	122.3(10)	124.266	120.638
Sn−Os−M[a]	92.4		
P(1)−Os−M[a]	57.4		
P(2)−Os−M[a]	165.2		
M−Os−H(01)[a]	88.3		
M−Os−H(02)[a]	100.0		
M−Os−H(03)[a]	108.7		

[a] M represents the midpoint of the C(1)−C(2) double bond.

values clearly support the trihydride character of **3**. Neither is there any interaction between the tin atom and the hydrides H(01) and H(03). The Sn−H(01) separations are 2.424 and 2.395 Å (**3a** and **3b**, respectively) and the Sn−H(03) distances are 2.500 (**3a)** and 2.528 Å (**3b**).

In agreement with the character of classic polyhydride of **3**, its IR spectrum in Nujol shows an Os−H absorption at 2019 cm^{-1}. In solution, complex **3** has a rigid structure only at low temperature. In accordance with this, the $^{31}P\{^1H\}$, $^{13}C\{^1H\}$, and ^1H NMR spectra are temperature dependent.

At 233 K, the $^{31}P\{^1H\}$ NMR spectrum in toluene-d_8 contains two doublets at 42.4 and 29.6 ppm with a P−P coupling constant of 119 Hz, and the corresponding tin satellites with P−Sn coupling constants of 116 (δ 42.4) and 162 (δ 29.6) Hz. This spectrum is fully consistent with the structure shown in Figure 3. On the basis of the Sn−Os−P(1) and Sn−Os−P(2) angles and the above-mentioned P−Sn coupling constants, the resonance at 42.4 ppm can be assigned to the phosphorus

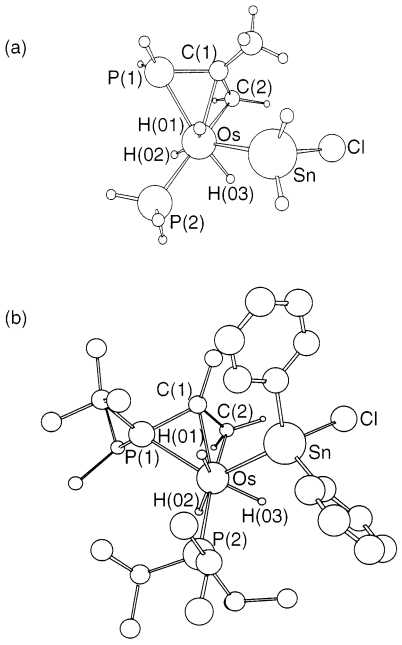

Figure 4. (a) B3LYP optimized structure of $OsH_3(SnH_2Cl)\{\eta^2\text{-}CH_2{=}C(CH_3)PH_2\}(PH_3)$ (**3a**) and (b) IMOMM (B3LYP:MM3) optimized structure of $OsH_3(SnPh_2Cl)\{\eta^2\text{-}CH_2{=}C(CH_3)P^iPr_2\}(P^iPr_3)$ (**3b**).

P(2), while the resonance at 29.6 ppm can be assigned to the phosphorus of the isopropenylphosphine P(1).

Raising the sample temperature leads to a decrease in the values of the P−P and P−Sn coupling constants in the resonance corresponding to P(2), whereas the resonance due to P(1) undergoes a broadening. At 313 K, the spectrum shows at 42.8 ppm a doublet with a P−P coupling constant of 84 Hz, along with the tin satellites ($J_{P-^{119}Sn} = J_{P-^{117}Sn} = 87$ Hz), and a very broad resonance between 20 and 27 ppm. These changes suggest that the constrained ring formed by the chelated isopropenylphosphine ligand and the osmium atom has a low stability. As a consequence, the coordinated olefinic C(1)−C(2) double bond is released at high temperature. The decoordination of this bond promotes the displacement of the phosphorus atom P(1) toward the equatorial plane of the bipyramid, decreasing the P(1)−Os−P(2) angle. The reduction of this angle gives rise to the observed decrease of the P−P coupling constant value, by increasing the temperature. At the same time, the movement of P(1) produces a light sliding of P(2) toward the tin atom, decreasing the Sn−Os−P(2) angle. The reduction of this angle is responsible for the observed decrease of the P−Sn coupling constant in the resonance due to P(2). The dynamic coordination−decoordination process undergone by the olefinic C(1)−C(2) double bond is also supported by the $^{13}C\{^1H\}$ and ^1H NMR spectra. At 233 K, the $^{13}C\{^1H\}$ NMR spectrum in toluene-d_8 contains three resonances due to the isopropenyl group of the phosphine. They appear at 50.4 (C(1)), 27.3 (C(2)), and 23.0 (C(3)) ppm, as doublets with C−P coupling constants of 17.9, 8.9, and 4.0 Hz, respectively. At 293 K, the resonances due to the C(1) and C(2) atoms are not observed. At 233 K, the ^1H NMR spectrum is consistent with the $^{13}C\{^1H\}$ NMR spectrum at this temperature. It contains three resonances for the

protons of the isopropenyl group of the phosphine at 2.66 (H trans to P), 2.56 (CH_3), and 2.16 (H cis to P) ppm. The last resonance appears as a broad signal, while the other ones are observed as doublets with H−P coupling constants of 29.6 (H) and 7.1 (CH_3) Hz. Rising the sample temperature leads to a broadening of the olefinic resonances, which disappear within the baseline at about 273 K. At about 293 K, they reappear. At 313 K, the spectrum shows two well-defined resonances for the olefinic protons of the isopropenyl group of the phosphine. They lie at 2.79 (H trans to P) and 2.29 (H cis to P) ppm, shifted about 0.13 ppm toward low field with regard to those observed at 233 K. These resonances appear as doublets with H−P coupling constants of 31.3 and 6.1 Hz, respectively.

In the high-field region, the ^{1}H NMR spectrum reveals another fluxional process. At 293 K, the spectrum shows a hydride resonance at about −10 ppm, with a 1:1 intensity ratio with regard to both resonances corresponding to the ortho-protons of the two inequivalent phenyl groups of the stannyl ligand. At 273 K, in addition to this resonance, a broad signal centered at about −11 ppm emerges from the baseline. At 233 K, the spectrum contains two double doublets at −9.93 and −11.00 ppm with H−P coupling constants of 18.9 and 19.8 and 21.2 and 22.0 Hz, respectively. These *r*esonances have a 2:1 intensity ratio. The first of them is assigned to the hydrides H(02) and H(03) and the second one to H(01). Because the chemical shift of the resonance due to H(02) and H(03) does not show significant changes with the temperature, we assume that the hydride H(01) does not exchange its position with the hydrides H(02) and H(03), at temperatures lower than 293 K. However, the presence of only one resonance for the inequivalent H(02) and H(03) hydrides indicates that, at temperatures higher than 233 K, these hydrides undergo a thermally activated exchange process that proceeds at rates sufficient to lead to the single hydride resonance. Consistent with this, lowering the sample temperature produces a broadening of the resonance. At 203 K, the decoalescence occurs. At 193 K, the spectrum contains three resonances at −9.80, −10.12, and −11.03 ppm with a 1:1:1 intensity ratio.

The T_1 values of the hydrogen nuclei of the OsH_3 unit of **3** were determined over the temperature range 273−210 K. At 300 MHz, $T_{1(min)}$ values of 215 ± 1 ms for H(02) and H(03) and 260 ± 1 ms for H(01) were obtained at 233 K. These values are in agreement with the trihydride character of **3**, and strongly support the above-mentioned assignment of the hydride resonances.

A broad singlet at 64.0 ppm in the ^{119}Sn{^{1}H} NMR spectrum at room temperature is also characteristic of **3**. We note that the tin chemical shift moves toward lower field as a result of the replacement of a phenyl group by a chlorine in these polyhydride systems. This is in contrast with the observation of Roper and coworkers for osmium(II)−trimethylstannyl complexes, where the tin chemical shift moves to higher field as methyl groups are replaced by iodide.[5h]

3. Synthesis and Characterization of $OsH_5(SnPh_2Cl)(P^iPr_3)_2$. In toluene under 1.5 atm of molecular hydrogen, complex **3** evolves into the osmium(VI)−pentahydride $OsH_5(SnPh_2Cl)(P^iPr_3)_2$ (**4**), as a result of the hydrogenation of the isopropenyl group of the phosphine and the oxidative addition of a hydrogen molecule to the osmium atom. Although complex **4** was formed in quantitative yield, according to eq 2, it was isolated as colorless microcrystals in only 27% yield, due to its high solubility in the usual solvents.

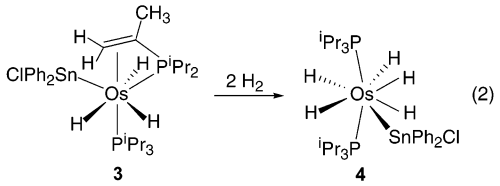

It should be pointed out that the reaction shown in eq 2 is another unusual d^4-d^2 oxidative addition process in platinum metal group chemistry. Furthermore, the different behavior of **1** and **3** toward molecular hydrogen should be noted.

Complex **4**, like **2** and **3**, was characterized by elemental analysis, IR, ^{1}H, ^{31}P{^{1}H}, ^{13}C{^{1}H}, and ^{119}Sn{^{1}H} NMR spectroscopy, and X-ray diffraction analysis. In this case at 173 K, the hydrogen atoms H(01), H(02), H(03), H(04), and H(05) were also located in the difference Fourier maps and refined as isotropic atoms together with the remaining non-hydrogen atoms of the structure. Figure 5 shows a view of the structure of this compound. Selected bond distances and angles are collected in Table 3.

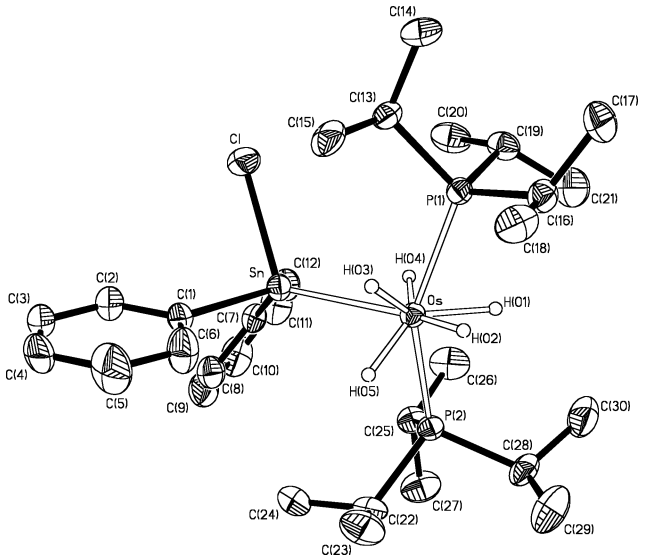

Figure 5. Molecular diagram of complex $OsH_5(SnPh_2Cl)(P^iPr_3)_2$ (**4**).

The coordination geometry around the osmium atom is like that of **2** with the hydride H(02) situated in the position of the chlorine atom of **2**; i.e., it can be rationalized as derived from a distorted dodecahedron with the hydride ligands H(03) and H(05) lying in the plane containing the phosphorus atoms of the phosphines.

The OsP_2Sn skeleton has a Y-shape, with the osmium atom situated in the common vertex, as in **2** and **3**. The angles P(2)−Os−P(1), P(2)−Os−Sn, and P(1)−Os−Sn are 149.31(3)°, 98.06(2)°, and 103.02(2)°, whereas the distances Os−P(1), Os−P(2), and Os−Sn are 2.3719(9), 2.3674(9), and 2.6261(3) Å, respectively.

Figure 6a shows the B3LYP optimized structure of $OsH_5(SnH_2Cl)(PH_3)_2$ (**4a**), while Figure 6b shows the

Table 3. Selected Bond Distances and Angles for the Complex $OsH_5(SnClPh_2)(P^iPr_3)_2$ (4) and Optimized Distances and Angles of $OsH_5(SnClH_2)(PH_3)_2$ (4a, B3LYP) and $OsH_5(SnClPh_2)(P^iPr_3)_2$ (4b, IMOMM (B3LYP:MM3)) (distances in Å, Angles in deg)

	4	4a	4b
Os−Sn	2.6261(3)	2.701	2.736
Os−P(1)	2.3719(9)	2.363	2.424
Os−P(2)	2.3674(9)	2.355	2.405
Os−H(01)	1.61(4)	1.654	1.643
Os−H(02)	1.33(5)	1.651	1.639
Os−H(03)	1.64(5)	1.640	1.632
Os−H(04)	1.59(4)	1.671	1.668
Os−H(05)	1.47(5)	1.644	1.634
Sn−Cl	2.4338(9)	2.412	2.415
Sn···H(05)		2.848	2.851
Sn···H(04)		2.514	2.513
Sn···H(03)		2.850	2.862
H(03)···H(05)		1.628	1.594
Sn−Os−P(1)	103.02(2)	94.232	103.022
Sn−Os−P(2)	98.06(2)	97.907	98.968
Sn−Os−H(01)	135.7(13)	139.461	140.052
Sn−Os−H(02)	152(2)	149.345	148.174
Sn−Os−H(03)	79.9(17)	77.783	77.332
Sn−Os−H(04)	65.6(16)	65.315	64.344
Sn−Os−H(05)	78.8(19)	77.794	76.904
P(2)−Os−P(1)	149.31(3)	153.300	148.450
P(1)−Os−H(01)	73.7(14)	77.245	72.943
P(1)−Os−H(02)	77(2)	91.135	85.963
P(1)−Os−H(03)	70.3(18)	73.382	74.956
P(1)−Os−H(04)	80.4(17)	81.983	85.639
P(1)−Os−H(05)	134(2)	132.834	132.439
P(2)−Os−H(01)	75.6(14)	78.079	75.654
P(2)−Os−H(02)	95(2)	90.420	87.159
P(2)−Os−H(03)	136.1(18)	132.465	132.524
P(2)−Os−H(04)	88.4(17)	81.658	83.788
P(2)−Os−H(05)	72(2)	73.258	74.515
H(01)−Os−H(02)	72(2)	71.107	71.756
H(01)−Os−H(03)	134(2)	134.037	135.252
H(01)−Os−H(04)	70(2)	74.227	75.706
H(01)−Os−H(05)	136(2)	136.083	135.677
H(02)−Os−H(03)	73(3)	74.921	75.692
H(02)−Os−H(04)	140(3)	145.327	147.446
H(02)−Os−H(05)	81(3)	76.496	74.739
H(03)−Os−H(04)	128(2)	133.582	131.594
H(03)−Os−H(05)	65(2)	59.464	58.404
H(04)−Os−H(05)	136(3)	131.587	131.648

IMOMM (B3LYP:MM3) optimized structure of **4** (**4b**). Their main geometrical parameters are collected in Table 3. The theoretical results agree well with those obtained from the X-ray diffraction analysis and indicate that the steric hindrance of the bulky ligands does not give rise to any distortion in the coordination polyhedron.

The separation between the hydride ligands is in all cases longer than 1.59 Å, whereas the separation between the tin atom and the hydride ligands is longer than 2.5 Å. The separations between the hydride ligands strongly support the pentahydride character of **4**, and the separations between the hydride ligands and the tin atom prove that there is no hydride−tin interaction. The structure of **4** is similar to that previously reported for $[OsH_5(P^iPr_3)_2(PR_3)]^+$ (R = $PHPh_2$, $P(OMe)Ph_2$).[11]

In agreement with the character of classic polyhydride of **4**, its IR spectrum in Nujol shows two bands at 2050 and 1971 cm^{-1}, corresponding to the Os−H vibrations. In the ^1H NMR spectrum in toluene-d_8, the most noticeable resonance is a triplet at −9.45 ppm with a H−P coupling constant of 9.6 Hz, along with the tin satellites ($J_{H-^{119}Sn} = J_{H-^{117}Sn} = 45$ Hz), corresponding to the hydride ligands. Lowering the sample temperature produces a broadening of the resonance. However, decoalescence is not observed upon 193 K. At 300 MHz, the T_1 values of this resonance were determined over the temperature range 253−223 K. In accordance with the pentahydride character of the complex, a $T_{1(min)}$ value of 130 ± 1 ms was obtained at 233 K.

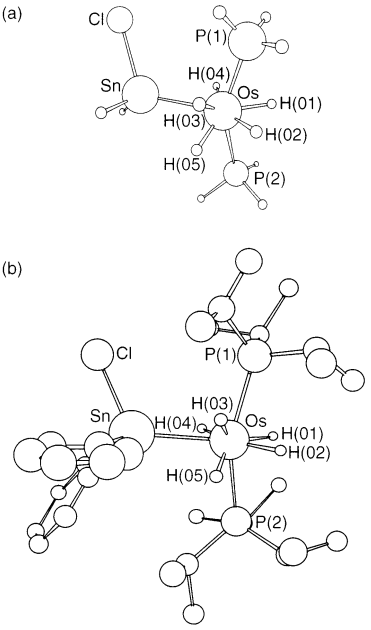

Figure 6. (a) B3LYP optimized structure of $OsH_5(SnH_2Cl)(PH_3)_2$ (**4a**) and (b) IMOMM (B3LYP:MM3) optimized structure of $OsH_5(SnPh_2Cl)(P^iPr_3)_2$ (**4b**).

At room temperature the $^{31}P\{^1H\}$ NMR spectrum shows a singlet at 46.9 ppm, along with the tin satellites ($J_{P-^{119}Sn} = J_{P-^{117}Sn} = 28$ Hz). Lowering the sample temperature produces a very light broadening of this resonance. Decoalescence is not observed upon 193 K.

A broad resonance at 68.1 ppm in the $^{119}Sn\{^1H\}$ NMR spectrum at room temperature is another characteristic feature of **4**. This chemical shift agrees well with that observed for **3**.

Concluding Remarks

This paper reveals the existence of the novel polyhydrides $OsH_4Cl(SnPh_3)(P^iPr_3)_2$, $OsH_3(SnPh_2Cl)\{\eta^2\text{-}CH_2{=}C(CH_3)P^iPr_2\}(P^iPr_3)$, and $OsH_5(SnPh_2Cl)(P^iPr_3)_2$, and shows the first d^4-d^2 oxidative additions of XY neutral molecules to platinum group metal complexes.

The dihydride−dichloro−osmium(IV) complex $OsH_2Cl_2(P^iPr_3)_2$ is one of the most fascinating species in modern osmium organometallic chemistry by its structure,[26] found in six-coordinate d^0-systems of zirconium and hafnium,[27] and by its reactivity.[28] It is now proven that is also capable of affording d^4-d^2 oxidative addition reactions. The reaction of this compound with $HSnPh_3$ leads to the d^2-tetrahydride $OsH_4Cl(SnPh_3)(P^iPr_3)_2$.

This tetrahydride allows access to other novel polyhydrides. In the presence of diphenylacetylene, it evolves

(26) (a) Aracama, M.; Esteruelas, M. A.; Lahoz, F. J.; López, J. A.; Meyer, U.; Oro, L. A.; Werner, H. *Inorg. Chem.* **1991**, *30*, 288. (b) Maseras, F.; Eisenstein, O. *New J. Chem.* **1998**, 5.

(27) Morse, P. M.; Girolami, G. S. *J. Am. Chem. Soc.* **1989**, *111*, 4114.

(28) Crochet, P.; Esteruelas, M. A.; López, A. M.; Martínez, M.-P.; Oliván, M.; Oñate, E.; Ruiz, N. *Organometallics* **1998**, *17*, 4500 and references therein.

into the trihydride compound $OsH_3(SnPh_2Cl)\{\eta^2\text{-}CH_2{=}C(CH_3)P^iPr_2\}(P^iPr_3)$ in a one-pot synthesis of multiple complex reactions, which has no precedent in organometallic chemistry. Under hydrogen atmosphere, it gives the pentahydride $OsH_5(SnPh_2Cl)(P^iPr_3)_2$, by another unusual d^4-d^2 oxidative addition reaction.

In conclusion, complex $OsH_2Cl_2(P^iPr_3)_2$ undergoes the d^4-d^2 oxidative addition of $HSnPh_3$ to give $OsH_4Cl(SnPh_3)(P^iPr_3)_2$, which is the entry to novel osmium−stannyl polyhydrides by means of unusual reactions, including a d^4-d^2 oxidative addition of hydrogen.

Experimental Section

All reactions were carried out under an argon atmosphere with Schlenk tube techniques. Solvents were dried and purified by known procedures and distilled under argon prior to use. The starting material $OsH_2Cl_2(P^iPr_3)_2$ (**1**) was prepared by a published method.[26] Infrared spectra were recorded on a Perkin-Elmer 883 spectrometer as solids (Nujol mull). ^1H, $^{13}C\{^1H\}$, $^{31}P\{^1H\}$, and $^{119}Sn\{^1H\}$ NMR spectra were recorded on either a Varian Gemini 2000, a Varian UNITY 300, or a Bruker AXR 300 instrument. Chemical shifts are referenced to residual solvent peaks (^1H, $^{13}C\{^1H\}$), external H_3PO_4 ($^{31}P\{^1H\}$), or external Me_4Sn ($^{119}Sn\{^1H\}$). Coupling constants J and N, ($N = J_{P-H} + J_{P'-H}$ for ^1H; $N = J_{P-C} + J_{P'-C}$ for $^{13}C\{^1H\}$), are given in hertz. C and H analyses were measured on a Perkin-Elmer 2400 CHNS/O analyzer.

Preparation of $OsH_4Cl(SnPh_3)(P^iPr_3)_2$ (2). A suspension of **1** (100 mg, 0.17 mmol) in 10 mL of toluene was treated with triphenyltin hydride (178.8 mg, 0.34 mmol). An immediate color change from brown to colorless was observed. The resulting solution was stirred for 2 min at room temperature and then evaporated to dryness. Addition of pentane affords a white solid that was washed repeatedly with pentane and dried in vacuo. Yield: 79 mg (52%). Anal. Calcd for $C_{36}H_{61}ClOsP_2Sn$: C, 48.03; H, 6.83. Found: C, 48.32; H, 6.32. IR (Nujol, cm^{-1}): ν(OsH) 2083 (s); ν(OsH) 1980 (s). ^1H NMR (300 MHz, tol-d_8, 293 K): δ 7.96 (d, $J_{H-H} = 6.9$, 6H, Ph−H_{ortho}), 7.18 (t, $J_{H-H} = 6.9$, 6H, Ph−H_{meta}), 7.09 (t, $J_{H-H} = 6.9$, 3H, Ph-H_{para}), 2.26 (m, 6H, PC*H*), 1.05 (dvt, $J_{H-H} = 6.9$, $N = 13.5$, 36H, PCH(CH_3)$_2$), −7.71 (br, 4H, OsH). $^1H\{^{31}P\}$ NMR (300 MHz, tol-d_8, 213 K, high field region): δ −2.92 (A part of an ABCC′XX′ spin system, 1H, Os−H), −5.92 (CC′ part of an ABCC′XX′ spin system, 2H, Os−H), −16.01 (B part of an ABCC′XX′ spin system, 1H, Os−H). $^{13}C\{^1H\}$ NMR (75.42 MHz, C_6D_6, 293 K): δ 146.9 (s, Ph), 137.7 (s with tin satellites, $J_{C-Sn} = 36$, Ph), 136.4 (s with tin satellites, $J_{C-Sn} = 47$, Ph), 130.5 (s, Ph), 129.3 (s, Ph), 127.8 (s, Ph), 26.5 (vt, $N = 29.4$, P*C*H), 19.4 (s, PCH(CH_3)$_2$). $^{31}P\{^1H\}$ NMR (121.42 MHz, tol-d_8, 293 K): δ 32.5 (s with tin satellites, $J_{P-Sn} = 20$).$^{119}Sn\{^1H\}$ NMR (111.83 MHz, C_6D_6, 293 K): δ −88.9 (br). T_1 (ms, OsH_4, 300 MHz, tol-d_8, 233 K): 175 ± 18 (−2.92 ppm), 169 ± 1 (−5.92 ppm), 171 ± 17 (−16.01 ppm). The mass spectrum (EI) of the mother liquors shows the presence of $ClSnPh_3$: m/z 385 (M^+), 309 (M^+ − Ph).

Preparation of $OsH_3(SnPh_2Cl)\{\eta^2\text{-}CH_2{=}C(CH_3)P^iPr_2\}(P^iPr_3)$ (3). A solution of **2** (300 mg, 0.33 mmol) in 10 mL of toluene was treated with diphenylacetylene (117 mg, 0.66 mmol). The resulting solution was stirred for 4 h at room temperature and then was evaporated to dryness. Addition of pentane affords a pale yellow solid that was washed with pentane and dried in vacuo. Yield: 133 mg (49%). Anal. Calcd for $C_{30}H_{53}ClOsP_2Sn$: C, 43.94; H, 6.51. Found: C, 43.65; H, 6.99. IR (Nujol, cm^{-1}): ν(Os−H) 2019 (m). ^1H NMR (300 MHz, tol-d_8, 313 K): δ 8.18 (d, $J_{H-H} = 7.3$, 2H, Ph−H_{ortho}), 7.80 (d, $J_{H-H} = 7.3$, 2H, Ph−H_{ortho}), 7.30 (t, $J_{H-H} = 7.3$, 2H, Ph−H_{meta}), 7.16 (d, $J_{H-H} = 7.3$, 2H, Ph−H_{meta}), 7.06 (t, $J_{H-H} = 7.3$, 2H, Ph−H_{para}), 2.80 (m, 1H, (CH_3)$_2$C*H*PC(CH_3)=CH_2), 2.79 (d, $J_{P-H} = 31.3$, 1H, PC(CH_3)=CH_{trans}), 2.44 (d, $J_{P-H} = 8.4$, 3H, PC(CH_3)=CH_2), 2.29 (d, $J_{P-H} = 6.1$, 1H, PC(CH_3)=CH_{cis}), 1.81 (m, 3H, PC*H*(CH_3)$_2$), 1.65 (m, 1H, (CH_3)$_2$C*H*PC(CH_3)=CH_2), 1.16−0.75 (m, 30 H, PCH(CH_3)), −9.96 (d, $J_{P-H} = 20.6$, 2H, Os−H). ^1H NMR (300 MHz, tol-d_8, 233 K, isopropenyl and hydride protons): 2.66 (d, $J_{P-H} = 29.6$, 1H, PC(CH_3)=CH_{trans}), 2.56 (d, $J_{P-H} = 7.1$, 3H, PC(CH_3)=CH_2), 2.16 (br, 1H, PC(CH_3)=CH_{cis}), −9.93 (dd, $J_{P-H} = 18.9$, $J_{P-H} = 19.8$, 2H, Os−H), −11.00 (dd, $J_{P-H} = 21.2$, $J_{P-H} = 22.0$, 1H, Os−H). $^{13}C\{^1H\}$ NMR (75.42 MHz, tol-d_8, 233 K): δ 154.4 (s, C_{ipso} $SnPh_2Cl$), 151.7 (s, C_{ipso} $SnPh_2Cl$), 131.8−124.7 (all s overlapping with the toluene-d_8 signals, Ph), 50.4 (d, $J_{P-C} = 17.9$, *C*=CH_2), 28.3 (d, $J_{P-C} = 22.7$, P*C*H(CH_3)$_2$), 27.4 (s, PCH(*C*H_3)$_2$), 27.3 (d, $J_{P-C} = 8.9$, C=*C*H_2), 23.0 (d, $J_{P-C} = 4$, C(*C*H_3)=CH_2), 19.8, 18.8, 17.02 (all s, PCH(*C*H_3)$_2$). $^{31}P\{^1H\}$ NMR (121.42 MHz, tol-d_8, 313 K): δ 42.8 (d with tin satellites, $J_{P-P} = 84$, $J_{P-Sn} = 87$), 20−27 (very broad). $^{31}P\{^1H\}$ NMR (121.42 MHz, tol-d_8, 233 K): δ 42.4 (d with tin satellites, $J_{P-P} = 119$, $J_{P-Sn} = 116$), 29.6 (d with tin satellites, $J_{P-P} = 119$, $J_{P-Sn} = 162$). $^{119}Sn\{^1H\}$ NMR (111.82 MHz, C_6D_6, 20°C): δ 64.0 (br). $T_{1(min)}$ (ms, OsH_3, 300 MHz, tol-d_8, 233 K): 215 ± 1 (−9.93 ppm), 260 ± 1 (−11.00 ppm).

Preparation of $OsH_5(SnPh_2Cl)(P^iPr_3)_2$ (4). Compound **3** (120 mg, 0.146 mmol) was placed in a 5-mm NMR tube provided with a Teflon closure and dissolved in toluene (2 mL). The argon atmosphere was replaced by an H_2 atmosphere. The progression of the reaction was followed by $^{31}P\{^1H\}$ NMR sprectroscopy and the NMR tube was periodically refilled with H_2 until complexion. The resulting brown solution was transferred to a Schlenk and evaporated to dryness. Addition of methanol afforded an off-white solid, which was washed with methanol and dried in vacuo. Yield: 32 mg (27%). Anal. Calcd for $C_{30}H_{57}ClOsP_2Sn$: C, 43.73; H, 6.97. Found: C, 43.44; H, 7.50. IR (Nujol, cm^{-1}): ν(OsH) 2050 (m), 1971 (m). ^1H NMR (300 MHz, tol-d_8, 293 K): δ 8.12 (d, $J_{H-H} = 6.6$, 4H, Ph−H_{ortho}), 7.28 (t, $J_{H-H} = 7.2$, 4H, Ph−H_{meta}), 7.15 (t, $J_{H-H} = 7.2$, 2H, Ph−H_{para}), 1.90 (m, 6H, PC*H*), 0.96 (dvt, $J_{H-H} = 7.2$, $N = 14.4$, 36H, PCH(CH_3)$_2$), −9.45 (t with tin satellites, $J_{P-H} = 9.6$, $J_{Sn-H} = 45$, 5H, Os−H). $^{13}C\{^1H\}$ NMR (75.42 MHz, C_6D_6, 293 K): δ 152.5 (s, Ph), 136 (s, Ph), 127.9 (s, Ph), 29.1 (vt, $N = 30.9$, P*C*H), 19.9 (s, PCH(*C*H_3)$_2$). $^{31}P\{^1H\}$ NMR (121.42 MHz, tol-d_8, 293 K): δ 46.9 (s with tin satellites, $J_{P-Sn} = 28$). $^{119}Sn\{^1H\}$ NMR (111.86 MHz, C_6D_6, 293 K): δ 68.1 (br). $T_{1(min)}$ (ms, OsH_5, 300 MHz, tol-d_8, 233 K): 130 ± 1 (−9.45 ppm).

Structural Analysis of Complexes 2, 3, and 4. X-ray data were collected for all complexes at low temperature on a Bruker Smart APEX CCD diffractometer at 173.0(2) K equipped with a normal focus, 2.4 kW sealed tube source (Molybdenum radiation, $\lambda = 0.71073$ Å) operating at 50 kV and 40 mA. Data were collected over the complete sphere by a combination of three or four sets. Each frame exposure time was 10 s covering 0.3° in ω. Data were corrected for absorption by using a multiscan method applied with the Sadabs[29] program. The structures for all compounds were solved by the Patterson method. Refinement, by full-matrix least squares on F^2 with SHELXL97,[30] was similar for all complexes, including isotropic and subsequently anisotropic displacement parameters for all non-hydrogen atoms. The hydrogen atoms were observed or calculated and refined freely or using a restricted riding model. Hydride ligands were located and refined with free positions and free or constrained thermal parameters. All the highest electronic residuals were observed in the close proximity of the Os centers and make no chemical sense. Crystal data and details of the data collection and refinement are given in Table 4.

(29) Blessing, R. H. *Acta Crystallogr.* **1995**, *A51*, 33−38. SADABS: Area-detector absorption correction, 1996, Bruker- AXS, Madison, WI.

(30) *SHELXTL* Package v. 6.10; Bruker-AXS: Madison, WI, 2000. Sheldrick, G. M. *SHELXS-86* and *SHELXL-97*; University of Göttingen: Göttingen, Germany, 1997.

Table 4. Crystal Data and Data Collection and Refinement for 2, 3, and 4

	2	3	4
		crystal data	
formula	$C_{36}H_{61}ClOsP_2Sn$	$C_{30}H_{53}ClOsP_2Sn$	$C_{30}H_{57}ClOsP_2Sn$
molecular wt	900.13	820.00	824.04
color and habit	colorless irregular block	yellow irregular block	colorless irregular block
symmetry, space group	triclinic, $P\bar{1}$	orthorhombic, $P2_12_12_1$	triclinic, $P\bar{1}$
a, Å	9.9811(11)	11.5559(8)	11.0122(9)
b, Å	11.3372(12)	13.7142(10)	11.2852(9)
c, Å	18.900(2)	20.9951(15)	15.3687(12)
α, deg	93.233(2)		90.238(1)
β, deg	99.814(2)		98.668(1)
γ, deg	113.757(2)		114.727(1)
V, Å^3	1910.2(3)	3327.3(4)	1710.2(2)
Z	2	4	2
D_{calc}, g cm^{-3}	1.565	1.637	1.600
		data collection and refinement	
diffractometer		Bruker Smart APEX	
λ(Mo Kα), Å		0.71073	
monochromator		graphite oriented	
scan type		ω scans	
μ, mm^{-1}	4.152	4.759	4.630
2θ, range deg	3, 57	3, 57	3, 57
temp, K	173	173	173
no. of data collect	18142	31275	21061
no. of unique data	8878 ($R_{int} = 0.0997$)	8003 ($R_{int} = 0.1394$)	8034 ($R_{int} = 0.0532$)
no. of params/restrains	396/0	359/4	347/0
R_1[a] [$F^2 > 2\sigma(F^2)$]	0.0513	0.0518	0.0288
wR_2[b] [all data]	0.0839	0.0747	0.0666
S[c] [all data]	0.732	0.698	1.037

[a] $R_1(F) = \sum||F_o| - |F_c||/\sum|F_o|$. [b] $\omega R_2(F^2) = \{\sum[\omega(F_o^2 - F_c^2)^2]/\sum[\omega(F_o^2)^2]\}^{1/2}$. [c] Goof $= S = \{\sum[(F_o^2 - F_c^2)^2]/(n - p)\}^{1/2}$, where n is the number of reflections, and p is the number of refined parameters.

Computational Details

DFT optimizations were carried out with the Gaussian98[31] series of programs, using the B3LYP functional.[32] A quasi-relativistic effective core potential operator was used to represent the innermost electrons of the osmium and tin atoms.[33] The basis set for the osmium and tin atoms was that associated with the pseudopotential with a standard valence double-ζ LANL2DZ contraction.[31] The d polarization function was added for the tin atom to supplement the standard basis.[34] A 6-31G(d) basis set was used for the phosphorus and chlorine atoms.[35] Hydrogens directly attached to the metal were described by using a 6-311G(p) basis set,[35] while a 6-31G basis set was used for the rest of the hydrogens.[34] A 6-31G basis set[35] was also used for all the carbon atoms, except for those involved in bonding with the osmium atom, which were described by using a 6-31G(d) basis set.[35] Calculations on the real systems were performed by using the IMOMM method,[36] with a program built from modified versions of two standard programs: Gaussian98[31] for the quantum mechanics part and mm3(92)[37] for the molecular mechanics part. The osmium atom and the atoms directly attached to it have been described at the QM level, while phosphine and stannyl substituents have been treated at the MM level. The QM part of the calculations was done at the B3LYP[32] level for the optimizations. The same basis sets as in the model complex calculations were used for real systems. The MM part of the calculations used the mm3-(92) force field.[38] van der Waals parameters for the osmium atom were taken from the UFF force field.[39] Torsional contributions involving dihedral angles with the metal were set to zero. All geometrical parameters were optimized, except the bond distances between the QM and MM regions of the molecule. The frozen values were 1.41 Å for the P−H bonds and 1.74 Å for the Sn−H bonds in the QM part and the crystallographic values for P−C and Sn−C bonds in the MM part.

Acknowledgment. We acknowledge financial support from the Spanish "Ministerio de Ciencia y Tecnología" and FEDER (Projects BQU2002-00606 and BQU2002-04110-CO2-02). The use of computational facilities of the Centre de Supercomputació de Catalunya is gratefully appreciated.

Supporting Information Available: Tables of positional and displacement parameters, crystallographic data, and bond lengths and angles. This material is available free of charge via the Internet at http://pubs.acs.org.

OM021038I

(31) Frisch, M. J.; Trucks, G. W.; Schlegel, H. B.; Scuseria, G. E.; Robb, M. A.; Cheeseman, J. R.; Zakrzewski, V. G.; Montgomery, J. A., Jr.; Stratmann, R. E.; Burant, J. C.; Dapprich, S.; Millam, J. M.; Daniels, A. D.; Kudin, K. N.; Strain, M. C.; Farkas, O.; Tomasi, J.; Barone, V.; Cossi, M.; Cammi, R.; Mennucci, B.; Pomelli, C.; Adamo, C.; Clifford, S.; Ochterski, J.; Petersson, G. A.; Ayala, P. Y.; Cui, Q.; Morokuma, K.; Malick, D. K.; Rabuck, A. D.; Raghavachari, K.; Foresman, J. B.; Cioslowski, J.; Ortiz, J. V.; Stefanov, B. B.; Liu, G.; Liashenko, A.; Piskorz, P.; Komaromi, I.; Gomperts, R.; Martin, R. L.; Fox, D. J.; Keith, T.; Al-Laham, M. A.; Peng, C. Y.; Nanayakkara, A.; Gonzalez, C.; Challacombe, M.; Gill, P. M. W.; Johnson, B. G.; Chen, W.; Wong, M. W.; Andres, J. L.; Head-Gordon, M.; Replogle, E. S.; Pople, J. A. *Gaussian 98*, revision A.6; Gaussian, Inc.: Pittsburgh, PA, 1998.

(32) (a) Lee, C.; Yang, W.; Parr, R. G. *Phys. Rev. B* **1988**, *37*, 785. (b) Becke, A. D. *J. Chem. Phys.* **1993**, *98*, 5648. (c) Stevens, P. J.; Devlin, F. J.; Chabalowski, C. F.; Frisch, M. J. *J. Phys. Chem.* **1994**, *98*, 11623.

(33) Hay, P. J.; Wadt, W. R. *J. Chem. Phys.* **1985**, *82*, 299.

(34) Höllwarth, A.; Böhme, M.; Dapprich, S.; Ehlers, A. W.; Gobbi, A.; Jonas, V.; Köhler, K. F.; Stegman, R.; Veldkamp, A.; Frenking, G. *Chem. Phys. Lett.* **1993**, *208*, 237.

(35) (a) Hehre, W. J.; Ditchfield, R.; Pople, J. A. *J. Chem. Phys.* **1972**, *56*, 2257. (b) Hariharan, P. C.; Pople, J. A. *Theor. Chim. Acta* **1973**, *28*, 213. (c) Francl, M. M.; Pietro, W. J.; Hehre, W. J.; Binkley, J. S.; Gordon, M. S.; DeFrees, D. J.; Pople, J. A. *J. Chem. Phys.* **1982**, *77*, 3654.

(36) Maseras, F.; Morokuma, K. *J. Comput. Chem.* **1995**, *16*, 1170.

(37) Allinger, N. L. *mm3(92)*; QCPE: Bloomington, IN, 1992.

(38) Allinger, N. L.; Yuh, Y. H.; Lii, J. H. *J. Am. Chem. Soc.* **1989**, *111*, 8551.

(39) Rappé, A. K.; Casewit, C. J.; Cowell, K. S.; Goddard, W. A., III; Skiff, W. M. *J. Am. Chem. Soc.* **1992**, *114*, 10024.